Received: 13 September 2019 | Revised: 9 January 2020 | Accepted: 10 January 2020

DOI: 10.1111/cas.14320

ORIGINAL ARTICLE

Cancer Science WILEY

Modulation of Nqo1 activity intercepts anoikis resistance and reduces metastatic potential of hepatocellular carcinoma

Masahiro Shimokawa | Tomoharu Yoshizumi | Shinji Itoh | Norifumi Iseda | Kazuhito Sakata | Kyohei Yugawa | Takeo Toshima | Noboru Harada | Toru Ikegami | Masaki Mori

Department of Surgery and Science, Graduate School of Medical Sciences, Kyushu University, Fukuoka, Japan

Correspondence
Shinji Itoh, Department of Surgery and Science, Graduate School of Medical Sciences, Kyushu University, Fukuoka City, Japan.
Email: itoshin@surg2.med.kyushu-u.ac.jp

Funding information
Japan Society for the Promotion of Science, Grant/Award Number: JP-16K10576 and 19K09198

Abstract

The processing of intracellular reactive oxygen species (ROS) by nuclear factor erythroid-derived 2-like 2 (Nrf2) and NADPH quinone oxidoreductase 1 (Nqo1) is important for tumor metastasis. However, the clinical and biological significance of Nrf2/Nqo1 expression in hepatocellular carcinoma (HCC) remains unclear. We aimed to clarify the clinical importance of Nrf2/Nqo1 expression in HCC and evaluate the association of Nrf2/Nqo1 expression with HCC metastasis. We also evaluated the impact of Nqo1 modulation on HCC metastatic potential. We used spheroids derived from HCC cell lines. In anchorage-independent culture, HCC cells showed increased ROS, leading to the upregulation of Nrf2/Nqo1. Futile stimulation of Nqo1 by β-lapachone induces excessive oxidative stress and dramatically increased anoikis sensitivity, finally diminishing the spheroid formation ability, which was far stronger than depletion of Nqo1. We analyzed 117 cases of primary HCC who underwent curative resection. Overexpression of Nrf2/Nqo1 in primary HCC was associated with tumor size, high α-fetoprotein, and des-γ-carboxy-prothrombin levels. Overexpression of Nrf2/Nqo1 was also associated with multiple intrahepatic recurrences (P = .0073) and was an independent risk factor for poor prognosis (P = .0031). NADPH quinone oxidoreductase 1 plays an important role in anchorage-independent survival, which is essential for survival for circulation and distant metastasis of HCC cells. These results suggest that targeting Nqo1 activity could be a potential strategy for HCC adjuvant therapy.

KEYWORDS

hepatocellular carcinoma, metastasis, Nqo1, Nrf2, oxidative stress

Abbreviations: β-Lap, β-lapachone; DCFDA, 2′,7′-dichlorofluorescein diacetate; GPx2, glutathione peroxidase-2; GSH, glutathione; GSSG, oxidized glutathione; HCC, hepatocellular carcinoma; HO1, hemoxidase-1; Keap1, Kelch-like ECH-associated protein 1; Nqo1, NADPH quinone oxidoreductase 1; Nrf2, nuclear factor erythroid-derived 2-like 2; p-Nrf2, phosphorylated Nrf2; ROS, reactive oxygen species.

1 | INTRODUCTION

Hepatocellular carcinoma is the second leading cause of cancer-related death worldwide and predominant in many countries such as France, Italy, Japan, and China.[1,2] Patients with HCC frequently suffer from intrahepatic or extrahepatic recurrence, which contribute to approximately 90% of HCC-related deaths.[3,4]

Cancer cells metastasize through several steps: detachment from the primary site, invasion through local tissue, intravasation into blood or lymph vessels, survival in circulation, extravasation, and formation of new tumors at distant sites.[5,6] When disengaging from the ECM and circulating in the bloodstream, cancer cells confront excessive oxidative stress[7-9] and need to acquire the ability to overcome ROS and detachment-induced apoptosis, also known as anoikis.[10]

Nuclear factor erythroid-derived 2-like 2 is a key transcription factor for processing intracellular ROS.[11] In the quiescent state, Keap1 and Cullin-3 interact with Nrf2 to facilitate ubiquitination and proteasomal degradation to keep high turnover with a short half-life of approximately 10-20 minutes.[12] Under oxidative stress, Keap1 senses ROS and releases Nrf2 to be stabilized and activated,[13] and under proliferative stress, the Raf/ Raf/ Myc pathway increases the transcription of Nrf2,[14] leading the regulation of increased ROS. Stabilized Nrf2 is phosphorylated at Ser40 by protein kinase C and translocated into the nucleus,[15] and subsequently binds to the antioxidant response elements to induce the expression of several antioxidants such as GPx2, HO1, and Nqo1. It has been also shown that Fyn kinase phosphorylates Tyr568 of Nrf2 that leads to export to the cytoplasm and degradation of Nrf2.[16]

Importantly, Nrf2 alters the intracellular metabolism and achieves high levels of NADPH synthesis that enables glutathione to process intracellular ROS.[17-19] NADPH quinone oxidoreductase 1 is a cytosolic detoxifying enzyme that maintains intracellular redox homeostasis by catalyzing quinones to hydroquinones with NADH and NADPH as electron donors.[20] Elevated tumor Nqo1 levels have led to the development of Nqo1-directed anticancer therapeutics, such as β-Lap and deoxyriboquinone.[21,22] β-Lapachone stimulates Nqo1 with a unique mechanism and shows tumor-suppressive effects by increasing intracellular ROS in cancer cells with high Nqo1 expression.[23,24] β-Lapachone (Q) is processed by Nqo1 and becomes unstable hydroquinones (QH_2), then immediately returns to original quinones (Q), releasing 2 molecules of superoxide. This Nqo1-dependent redox cycling is reported to oxidize 60 mol NAD(P)H, creating 120 mol ROS within 2 minutes and deliver DNA damage and cell death.[25] At the same time, Nqo1 consumes massive amounts of NADPH in repeatedly processing β-Lap, accompanied by further ROS production through the repeated reduction of NADP+. Thus, β-Lap stimulates the upregulated Nqo1 enzyme and increases the excessive ROS production, just like revving up the idling engine and increasing the exhaust CO_2 gas. Finally, unlike ordinal Nqo1 activation that lowers ROS, β-Lap increases excessive ROS and induces apoptosis or anoikis. Notably, β-lapachone has been found to suppress the metastasis of lung cancer,[24] further supporting its anti-metastasis effect.

Some retrospective studies have reported that Nrf2 and Nqo1 contribute to tumor invasiveness and drug resistance through regulating ROS or metabolic rearrangement in several cancers.[14,26,27] Moreover, Nqo1 has been recently reported to be responsible for poor prognosis of HCC[28] and other cancers.[22,29] However, the association of Nqo1 expression with postoperative recurrence or distant metastasis of HCC has not been investigated.

The aim of this study was to examine whether Nqo1 functions in regulating anoikis of human HCC cells. We also evaluated the potential association between Nqo1 expression and HCC recurrence through clinicopathological analysis.

2 | MATERIALS AND METHODS

2.1 | Reagents

The DCFDA Cellular ROS Detection Assay Kit (Abcam), Calorimetric GSH/GSSG Assay kit, NADP+/NADPH Assay kit (Cell Biolabs), CCK-8 (Dojindo), and the Apoptosis/ Necrosis Assay Kit (Abcam) were used in this study. The Nqo1 stimulator β-Lap (3,4-dihydro-2,2-dimethyl-2H-naphtho[1,2-b]pyran-5-6-dione) was purchased from Sigma-Aldrich. Antibodies against Keap1, phosphorylated Nrf2 (Ser40), and Nqo1 were purchased from Abcam. Anti-GPx Abs were obtained from Cell Signaling Technology. Anti-β-actin Ab was obtained from Sigma-Aldrich. Stealth RNAi (Thermo Fisher Scientific) and GIPZ Lentiviral shRNA (GE Healthcare Dharmacon) were used for knocking down *Nrf2*, *Nqo1*, and *Keap1* genes.

2.2 | Two-dimensional/3D cell culture and gene suppression

Hepatocellular carcinoma cell lines were obtained from the Japanese Cancer Research Resources Bank (JCRB) Cell Bank (Osaka, Japan) and were confirmed to be free from mutations in *KEAP1*, *NFE2L2*, and *NQO1* genes using the database of the Cancer Dependency Map (https://depmap.org/portal/); PLC/PRF5 (Cell ID, JCRB 0406; Depmap ID, ACH-001318; https://depmap.org/portal/cell_line/PLCPRF5_LIVER?tab=mutation) and HuH7 (Cell ID, JCRB 0403; Depmap ID, ACH-000480; https://depmap.org/portal/cell_line/ACH-000480?tab=mutation). Cells were cultured in DMEM with 10% FBS and 1% L-glutamine at 37°C at 10% CO_2. For suspended culture, cells were filtered with a 40 μm cell strainer (Corning) and seeded in EzSphere plates (Asahi Glass Company) or Ultra-Low Attachment Microplates (Corning) with low-adhesion coatings.

In addition to Nqo1 knockdown cells, we used Keap1 knockdown cells to promote Nrf2 activation in response to ROS. Transient gene suppression was achieved in PLC and HuH7 HCC cells, using Stealth RNAi. Cells were prepared in complete growth medium without antibiotics so that 500 μL contains 50 000 cells (30%-50% confluence 24 hours after plating). Then reverse transfection was carried out using 10 nmol/L Stealth RNAi with Opti-MEM I Reduced

Serum Medium and Lipofectamine RNAiMAX for 24 hours at 37°C in a CO_2 incubator. Stable gene silencing was carried out using GIPZ Lentiviral shRNA (GE Healthcare Dharmacon). After overnight incubation of 50 000 cells/well in 24-well plates, 25 µL diluted shRNA lentivirus (preadjusted functional titer = 0.8-1.2 × 10^6 TU/mL) was added and cultured with serum-free medium for 6 hours. Following 72 hours of transduction time with serum-containing medium, puromycin selection was undertaken at 5 µg/mL concentration and single cell lines were established through 14 days of selection.

2.3 | Immunocytochemical staining

Immunocytochemical staining was carried out on attached cells and spheroids. Cells were seeded onto small coverslips in 2-well plates and incubated at 37°C for 24 hours to allow cell attachment. Spheroids were harvested 24 hours after seeding in low-adhesion conditions and affixed with SmearGell (GenoStaff) prior to methanol fixation. The cells were fixed with 90% methanol at 4°C for 20 minutes and permeabilized with 0.1% Triton X-100 for 10 minutes, followed by incubation in 3% BSA at room temperature for 30 minutes. The blocking buffer was removed, and the cells were incubated with primary Abs at 4°C for 1 hour. After washing with PBS, cells were incubated with fluorescence-conjugated secondary Abs for 1 hour. DNA was counterstained with UltraCruz Mounting Medium containing DAPI (Santa Cruz Biotechnology). The slides were viewed with a BZ-9000 fluorescence microscope (Keyence).

Intensity of immunocytochemical staining was measured using ImageJ for 5 fields of view. Images were converted into grayscale and the threshold was adjusted to highlight the area of the cells for analysis. Integrated density of the defined area was measured and the area of the object in the entire image was quantified by the average pixel intensity. The intensity of the object is the quotient of integrated density and measured object area. The intensities of each target protein were normalized to those of nucleotide (DAPI).

2.4 | Western blot analysis

Protein lysates were separated by 10% SDS-PAGE with Mini-PROTEAN TGX gels (Bio-Rad) and transferred onto a PVDF membrane using the Trans-Blot Turbo Transfer System (Bio-Rad).[30] Western blot analysis was processed on the iBind Western System (Thermo Fisher Scientific) for 6 hours at room temperature according to the manufacturer's protocol. Protein bands were visualized with HRP-conjugated secondary Abs and Chemi-Lumi One (Nacalai Tesque) on an Amersham Imager 600 (GE Healthcare).

2.5 | Reactive oxygen species analysis

Reactive oxygen species analysis was carried out using the DCFDA Cellular Reactive Oxygen Species Detection Assay Kit (ab113851; Abcam) according to the manufacturer's protocol.[31] A total 25 000 cells per well (for both adherent culture and suspended culture conditions) were seeded on a 96-well plate and incubated at 37°C for 24 hours in 10% CO_2. Cells were then stained with 20 µmol/L of DCFDA at 37°C for 30 minutes (suspension cells) or 45 minutes (adherent cells). Signals of oxidized DCF at 485/535 nm Ex/Em were read on a Synergy H1 fluorescent plate reader (BioTek).

2.6 | Intracellular GSH/GSSG ratio measurements

The intracellular GSH/GSSG ratio was determined with the OxiSelect Total Glutathione (GSSG/GSH) Assay Kit (STA-312; CellBiolabs), according to the manufacturer's protocol. Harvested cells were centrifuged and resuspended with 250 µL ice-cold 5% metaphosphoric acid at a concentration of 2 × 10^6 cells and homogenized. The supernatant was filtered with a 10 kDa spin filter for deproteination and tested immediately for total GSH/GSSG quantification. Next, 100 µL of the samples were mixed with 25 µL glutathione reductase solution, 25 µL NADPH solution, and 50 µL chromogen solution. The absorbance at 405 nm was measured with a Multiskan GO spectrophotometric microplate reader (Thermo Fisher Scientific).

2.7 | Intracellular NADP+/NADPH ratio measurements

The intracellular NADPH level and NADP+/NADPH ratio were determined using the Calorimetric NADP+/NADPH Assay Kit (Cell Biolabs), according to the manufacturer's protocol. Harvested cells were resuspended at 2 × 10^6 cells/mL in extraction buffer and homogenized on ice. The supernatant was filtered with a 10 kDa spin filter for deproteination and total NADP+/NADPH quantification was immediately carried out. Extraction of NADPH and NADP+ included the addition of NaOH and HCl to eliminate NADP+ and NADPH, respectively, followed by incubation at 80°C for 1 hour and pH neutralization. Samples were then mixed with NADP Cycling Reagent and incubated for 2 hours at room temperature protected from light. The NADP+/NADPH concentrations were calculated by comparing the sample optical density read with a Multiskan GO spectrophotometric microplate reader at 450 nm.

2.8 | Cell viability assays

Cell viability was determined using the CCK-8 (Dojindo) following the manufacturer's protocol. Briefly, 5000 cells in 100 µL per well were plated in a 96-well plate along with a control well with no cells. Cells were cultured in 10 µL medium containing various concentrations of Nqo1 bioactivator and then incubated in CO_2 for 24 hours. Next, 10 µL water-soluble tetrazolium solution was added to each well and cells were incubated for 1 hour. Absorbance was measured through a 450 nm filter on a Multiskan GO spectrophotometric microplate reader.

2.9 | Apoptosis and necrosis detection assays

The Apoptosis/Necrosis Detection Kit (ab176749; Abcam) was used to evaluate anoikis. Briefly, cells were seeded at a density of 1×10^5 cells/mL in a 6-well plate with low-adhesion coating and incubated for 48 hours at 37°C. Spheroids were attached to the bottom of the plate by centrifuging and the supernatant was discarded. After staining with 204 μL assay buffer containing Apopxin, 7-AAD, and CytoCalcein, spheroids were analyzed under a BZ-9000 fluorescent microscope (Keyence). Apoptotic and necrotic cells were indicated with green staining using the FITC channel (Ex/Em = 490/525 nm) and red staining using the Texas Red channel (Ex/Em = 550/650 nm), respectively.

2.10 | Anchorage-independent growth assays

PLC and HuH7 cells were cultured in low-adhesion coated 6-well EzSphere plates (Asahi Glass Company) at 500 cells/mL in culture medium. Two milliliters was added to each well and placed still without oscillation. A total of 250-500 mL new culture media was added every 2 days. Plates were imaged after 2 and 7 days using an Olympus IX70 inverted microscope. The number of spheroids in each well was quantified using ImageJ software (https://imagej.net/).

2.11 | Tissue samples

Tumorous and adjacent nontumorous liver tissues were collected from 127 patients who had undergone curative surgery for primary HCC between 2004 and 2009 at the Department of Surgery and Science, Kyushu University Hospital. Specimens were also collected when patients had undergone curative resection or tissue sampling for recurrent and metastatic lesions. The differential diagnosis for intrahepatic recurrences and de novo lesions (ie, multicentric HCC) was morphologically carried out by 2 liver pathologists. Informed consent was obtained from each patient and the study protocol conforms to the ethical guidelines of the 1975 Declaration of Helsinki. This study was approved by the institutional review board, the Center of Clinical and Translational Research of Kyushu University (Number: 27-294).

2.12 | Immunohistochemical analysis

Tissue samples were fixed with 10% buffered formalin. Immunohistochemical staining for p-Nrf2 and Nqo1 were carried out on paraffin-embedded sections (4 μm thickness).[20] Capture of light microscopic images and quantitative analysis were undertaken on the NanoZoomer platform (Hamamatsu Photonics). The positivity of p-Nrf2 staining was defined when the stained nucleus count was 50% or more in at least in 5 fields of view.

2.13 | Gene expression analysis

Total RNA was extracted from cultured cells or surgically obtained tissues using the Maxwell RSC Instrument (Promega) and reverse-transcribed using SuperScriptIII (Invitrogen) following the manufacturers' instructions. Quantitative RT-PCR was undertaken using TaqMan Universal PCR Master Mix (Thermo Fisher Scientific) and the ABI Prism 7000 Sequence Detection Systems (Applied Biosystems). The relative mRNA amounts were determined using the *β-actin* gene as reference. Briefly, we normalized each set of samples using the difference in threshold cycles (ΔCT) between the targeted gene and β-actin gene ($\Delta CT_{sample} = \Delta CT_{target} - \Delta CT_{\beta\text{-actin}}$). cDNA from the tissue sample, which expressed both NQO1 and β-actin mRNAs, was used as the calibration sample ($\Delta CT_{calibration}$). Relative mRNA levels were calculated by $2^{-\Delta\Delta CT}$, where $\Delta\Delta CT = \Delta CT_{sample} - \Delta CT_{calibration}$.

2.14 | Statistical analysis

Statistical differences were determined using Student's *t*-test or the Mann-Whitney test. Multivariate logistic regression analysis was also carried out for patient survival analysis. All statistical analyses were undertaken using JMP software (version 13.0; SAS Institute). *P* values less than 0.05 were considered significant.

3 | RESULTS

3.1 | Phosphorylated Nrf2 and Nqo1 were observed in HCC spheroids

To generate early spheroids, PLC and HuH7 HCC cell lines were seeded and harvested after 48 hours of incubation in low-adhesion plates (Figure 1A). In spheroid culture, immunocytochemical staining showed that p-Nrf2 and Nqo1 protein expression were induced strongly in the nucleus and cytoplasm, respectively (Figure 1A). Relative fluorescence intensities of p-Nrf2 and Nqo1 in both monolayer and spheroid culture are shown in Figure S1A. We also investigated mRNA and protein expression of Nrf2 and its downstream antioxidant targets. The expressions of p-Nrf2, GPx2, and Nqo1 were induced in spheroid culture (Figure 1B,C).

3.2 | Anchorage-independent culture increased intracellular oxidative stress

Higher levels of ROS were observed in spheroid culture compared with monolayer culture (Figure 1D). Lower GSH/GSSG ratios, indicating the consumption of reduced GSH and accumulation of GSSG, were observed in spheroid culture (Figure S1B). Elevated NADPH was observed in spheroid culture (Figure S1C), implying promoted NADPH synthesis as a result of Nrf2 activation and intracellular metabolic alteration. Higher NADP+/NADPH ratios were also observed (Figure

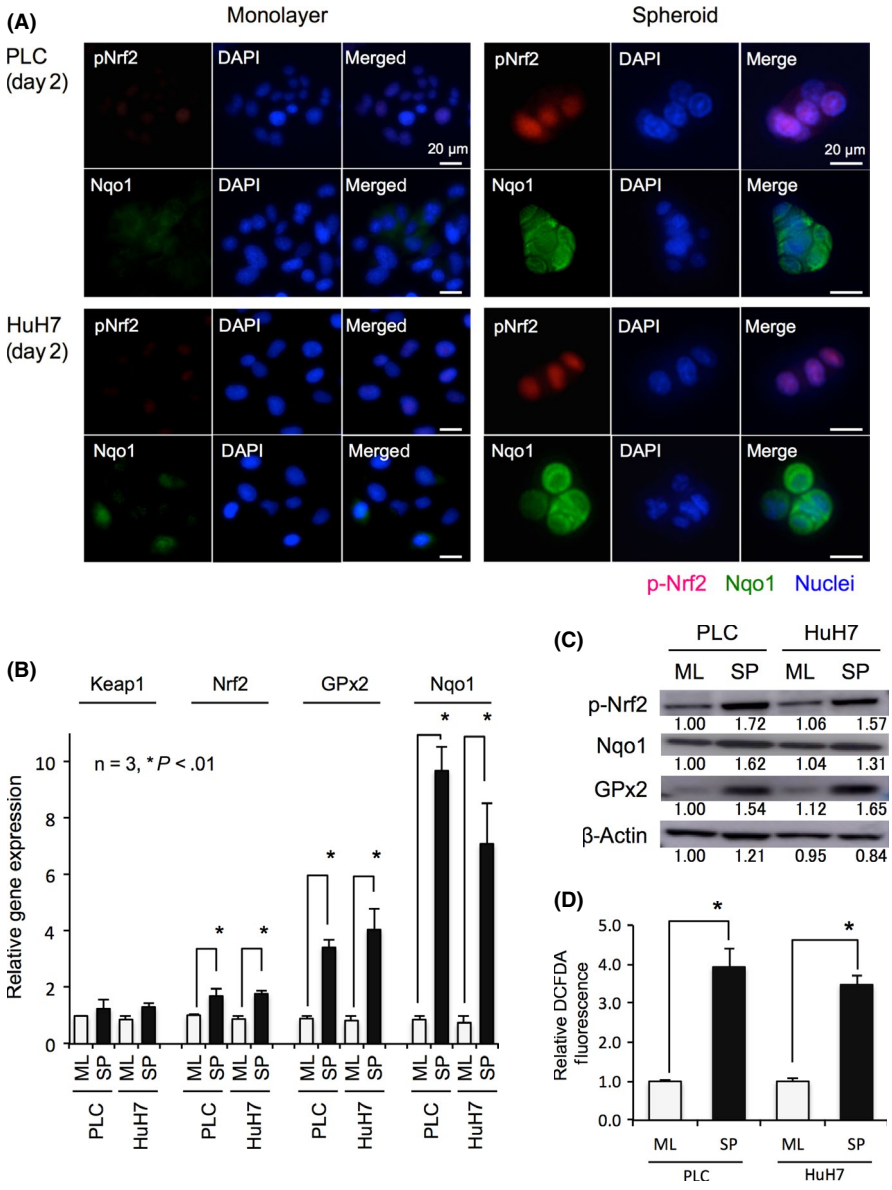

FIGURE 1 Antioxidant response in anchorage-independent culture of hepatocellular carcinoma cells. A, Examples of immunocytochemical staining of early spheroid culture (day 2). Elevated Ser40 phosphorylated nuclear factor erythroid-derived 2-like 2 (p-Nrf2) and NADPH quinone oxidoreductase 1 (Nqo1) protein expressions were detected in nucleus and cytoplasm, respectively. Scale bar = 20 μm. B, C, Relative mRNA expression (B) and protein expression (C) of Kelch-like ECH-associated protein 1 (Keap1), Nrf2, glutathione peroxidase-2 (GPx), and Nqo1 in monolayer (ML) and spheroid (SP) culture. Nrf2 and its target proteins, Nqo1 and GPx, were increased in spheroid culture. Protein levels are indicated below each image. D, Intracellular oxidative stress in ML and SP culture. Reactive oxygen species levels indicated by the relative 2′,7′-dichlorofluorescein diacetate (DCFDA) fluorescence intensity increased in spheroid culture. All data represent means ± SEM of 3 experiments. *P < .01

S1D), which indicates that NADPH was converted into NADP+ for the reduction of GSSG to GSH.

3.3 | NADPH quinone oxidoreductase 1 essential for ROS reduction and spheroid formation

In monolayer culture, it was confirmed that the Nrf2/Nqo1 axis is responsible for ROS tolerance. Knockdown of Keap1 increased p-Nrf2 levels without affecting its gene expression, and also significantly induced Nqo1 gene and protein expression (Figure 2A,B). Staining of spheroids with DCFDA at day 2 showed that oxidative stress was excessive in Nrf2 knockdown cells and Nqo1 knockdown cells, whereas Keap1 suppression reduced ROS levels (Figure 2C, P < .01). Knockdown of Nrf2 or Nqo1 significantly reduced cell viability against oxidative stress in monolayer culture (Figure S2).

Results of the apoptosis/necrosis detection assay of spheroids at day 2 are shown in Figure 3A,B. Suppression of Keap1 tended to reduce the rate of apoptosis and necrosis as indicated with Apopxin and 7-AAD, respectively. Depletion of Nrf2 or Nqo1 severely attenuated HCC cell survival in anchorage-independent conditions. Spheroid images and size distributions for day 7 are shown in Figure 3C,D. Depletion of Nqo1, as well as Nrf2 suppression, significantly reduced the size and number of HCC spheroids at day 7, whereas suppressing Keap1 enhanced spheroid formation.

3.4 | β-Lapachone increased intracellular ROS and reduced HCC spheroid formation

We next used the Nqo1 stimulator β-Lap on spheroid culture of control cells and Nqo1 knockdown cells (Figure S3). Consistent with a previous study, 5 μmol/L β-Lap remarkably increased intracellular ROS in spheroids with overexpressing Nqo1, but not with Nqo1 knockdown cells (Figure 4A). In anchorage-independent culture with Nqo1 active cells, β-Lap dose-dependently decreased the cell

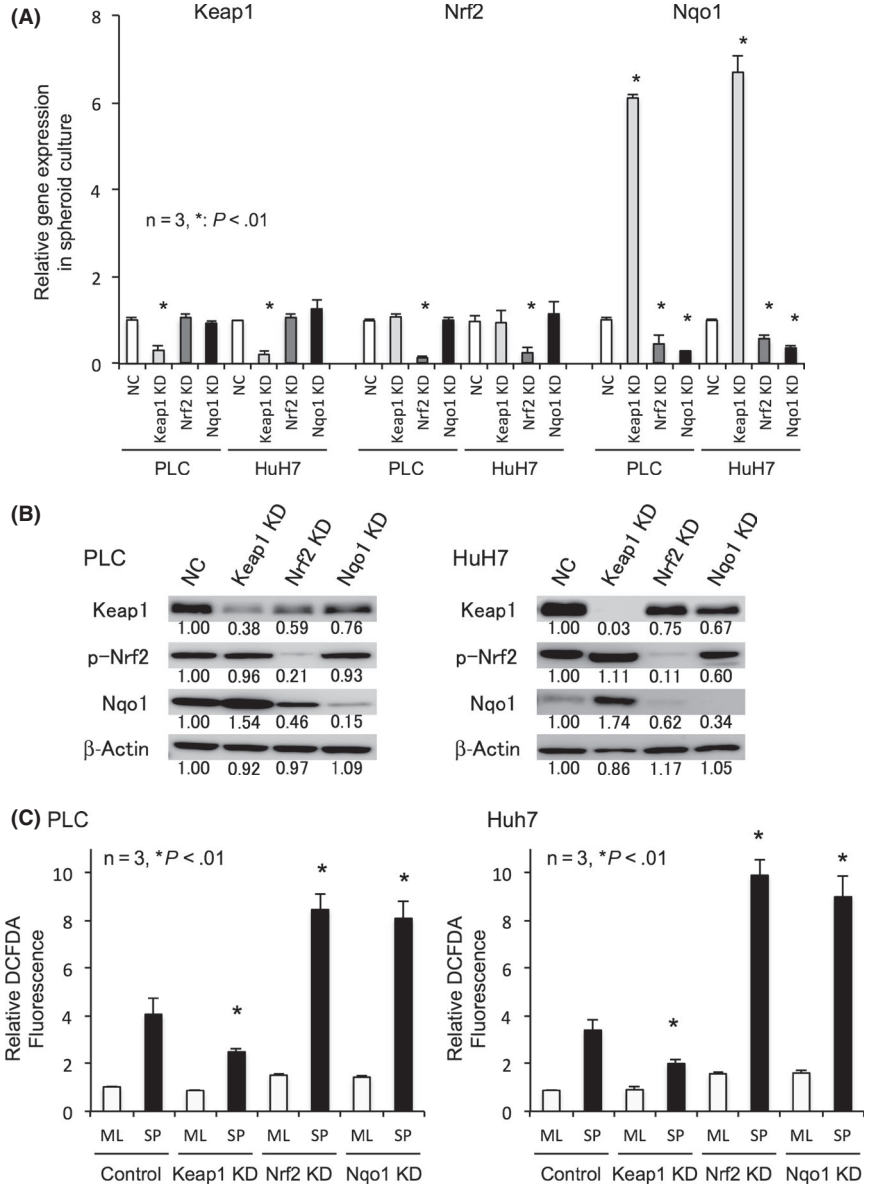

FIGURE 2 Depletion and induction of NADPH quinone oxidoreductase 1 (Nqo1) changes the intracellular reactive oxygen species (ROS) levels. A, B, Relative mRNA expression (A) and protein expression (B) of nuclear factor erythroid-derived 2-like 2 (Nrf2)-related antioxidants in spheroid culture of negative control (NC), Kelch-like ECH-associated protein 1 (Keap1), Nrf2, and Nqo1 transient knockdown (KD) cells. Keap1 KD induced Nqo1 expressions, while Nrf2 KD decreased Nqo1 expressions in spheroid culture. Protein levels are indicated below each image. C, Intracellular oxidative stress in monolayer (ML) and spheroid (SP) culture of control, Keap1, Nrf2, and Nqo1 knockdown cells. ROS levels indicated by the relative 2′,7′-dichlorofluorescein diacetate (DCFDA) fluorescence intensity decreased in Keap1 KD cells but increased in Nrf2 or Nqo1 KD cells in spheroid culture. All data represent means ± SEM of 3 experiments. *$P < .01$

viability, which was cancelled by ameliorating ROS by the addition of N-acetyl-L-cysteine (Figure 4B). Spheroid formation was diminished by administration of β-Lap, and decreasing ROS by addition of N-acetyl-L-cysteine recovered the ability of spheroid formation (Figure 4C).

3.5 | Enhanced expression of Nqo1 was correlated with intrahepatic recurrence and poor prognosis in human HCC

To determine whether elevated Nqo1 expression confers a survival disadvantage in HCC, we analyzed gene expression and survival data from HCC patients who underwent curative hepatectomy in our institute. Immunohistochemical staining of primary HCC samples revealed the expression of p-Nrf2 in the nucleus and Nqo1 in the cytoplasm (Figure 5A). To avoid deceptive quantification due to insufficient discrimination between cytoplasmic Nqo1 staining and nonspecific staining, mRNA-based classification was adopted. Patients were stratified into high and low Nqo1 expression groups based on a quartile-bound cut-off; a total of 31 patients were categorized in the high Nqo1 expression group and 87 patients were categorized in the low Nqo1 expression group (Figure 5B). The correlation between p-Nrf2 immunohistochemical staining and Nqo1 mRNA expression is shown in Figure S4A.

There was no significant difference between the 2 groups in terms of patient background, such as etiology of HCCs, liver function indicators, and fibrosis scores. High Nqo1 expression was associated with aggressive clinicopathologic features of HCC including elevated α-fetoprotein and protein induced by vitamin K absence/antagonist II values, large tumor sizes, and venous invasion (Table 1). Of note, among 76 cases with intrahepatic recurrence, patients in the Nqo1 high expression group showed a

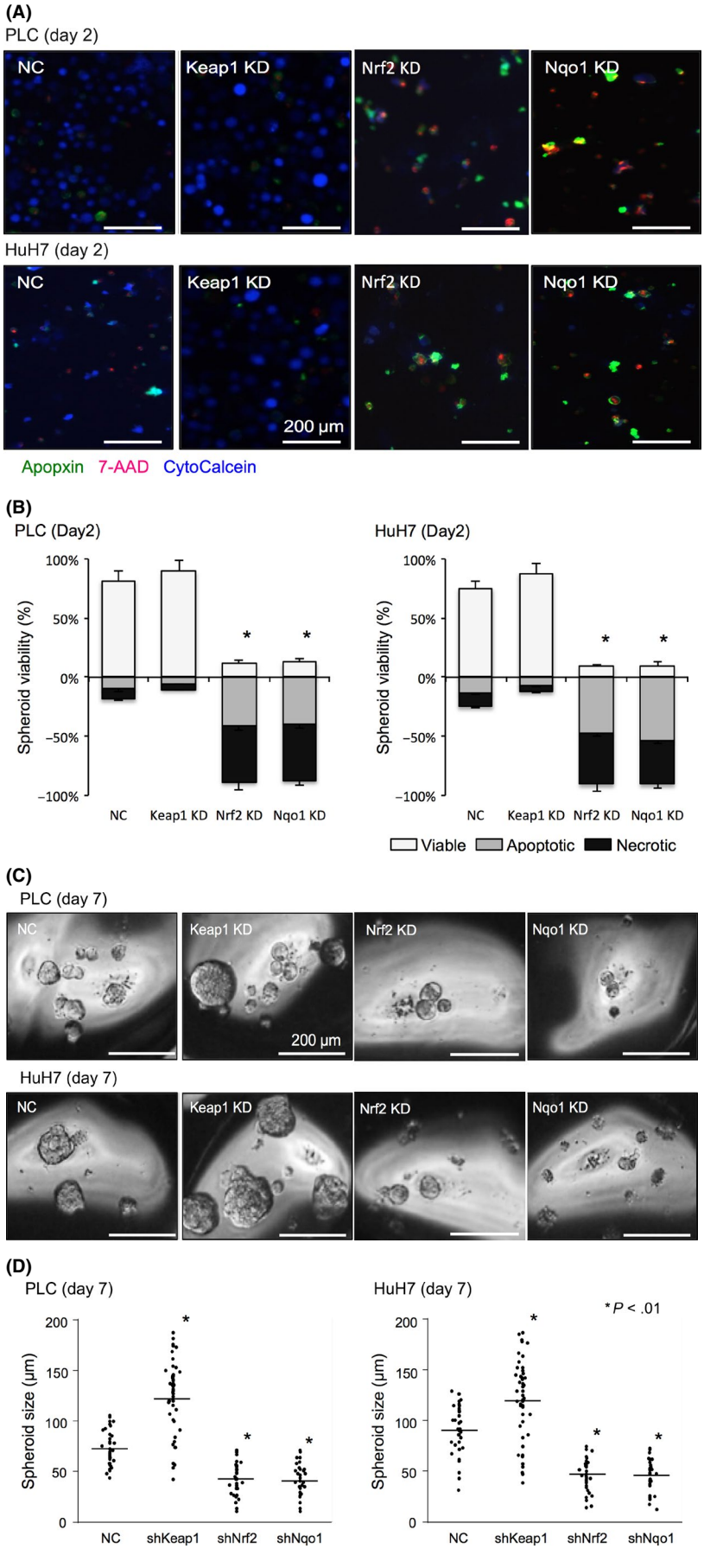

FIGURE 3 Depletion and induction of NADPH quinone oxidoreductase 1 (Nqo1) alter the sensitivity of hepatocellular carcinoma cells to anoikis. A, Representative images of apoptosis/necrosis detection assay for spheroid culture on day 2 from control, Kelch-like ECH-associated protein 1 (Keap1), nuclear factor erythroid-derived 2-like 2 (Nrf2), and Nqo1 knockdown cells. Apopxin (green), 7-AAD (red), and CytoCalcein (blue) indicate apoptosis, late apoptosis and necrosis, and viable cells, respectively. Scale bar = 200 μm. B, Graphical presentations for the proportions of viable, apoptotic, and necrotic spheroids from apoptosis/necrosis detection assays (A). Keap1 KD tended to decreased apoptosis/necrosis, whereas Nrf2 or Nqo1 KD significantly decreased viability in early detachment culture. C, Representative images of spheroids on day 7 from control, Keap1, Nrf2, and Nqo1 knockdown cells. Scale bar = 200 μm. D, Distribution of size and number of spheroids from control, Keap1, Nrf2, and Nqo1 knockdown cells. Keap1 KD significantly increased the sphere size and number of spheroids, whereas Nrf2 or Nqo1 KD significantly decreased them. Lines indicate the average values for each data points. All data represent means ± SEM of 3 experiments. *$P < .01$

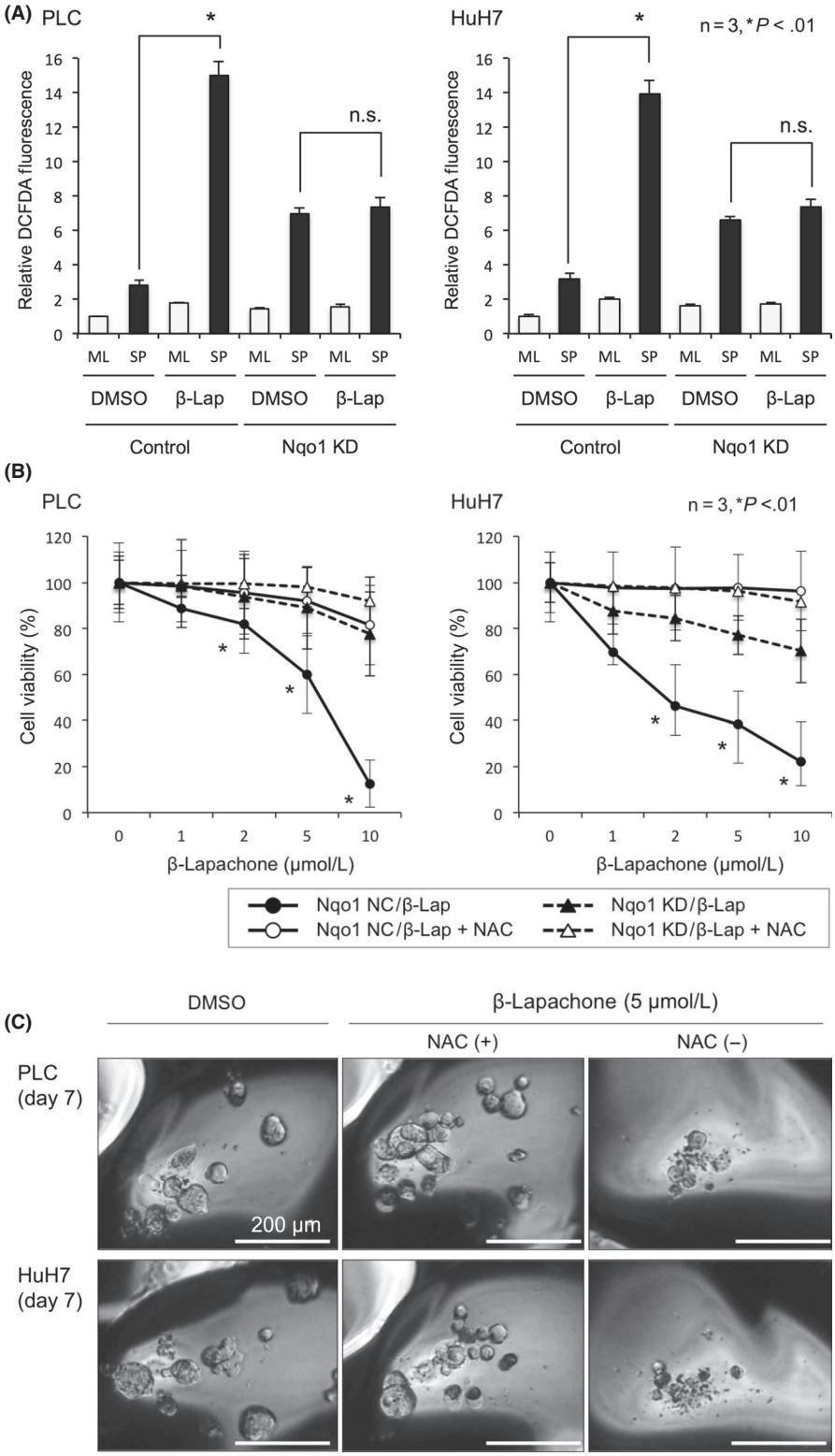

FIGURE 4 β-Lapachone (β-Lap) increases reactive oxygen species (ROS) and reduces spheroid formation in hepatocellular carcinoma cells. A, Intracellular oxidative stress in monolayer (ML) and spheroid (SP) culture of control and NADPH quinone oxidoreductase 1 (Nqo1) knockdown (KD) cells. ROS levels are indicated by the relative 2′,7′-dichlorofluorescein diacetate (DCFDA) fluorescence intensity. β-Lap treatment increased intracellular ROS approximately 5-fold in spheroid culture of control cells, but did not in Nqo1 knockdown cells. B, β-Lap dose-dependently decreased cell viability in suspended culture at 48 h in detached culture cells with active Nqo1, which was ameliorated by addition of N-acetyl-L-cysteine (NAC). C, Representative images of spheroids treated with β-Lap alone or with NAC. All data represent means ± SEM of 3 experiments. *P < .01. Scale bar = 200 μm. NC, control; DMSO, imethyl sulfoxide

higher incidence (72.2% vs 36.2%, P = .0073) of multiple recurrent lesions (Figure 5C). Furthermore, HCC patients with high tumor Nqo1 expression levels showed a worse overall survival (P = .013), although there was no significant difference in recurrence-free survival (P = .28) (Figure 5D,E). Univariate and multivariate analysis revealed that high Nqo1 expression was an independent risk factor for poor prognosis (risk ratio 3.02, P = .0031), as well as intrahepatic metastasis at primary hepatic resection (risk ratio 3.94, P = .0021). The prognosis was not affected by low liver function, defined when patients meet more than 2 of the following criteria: serum total bilirubin, 2.0 mg/dL or higher; albumin, 3.5 g/dL or less; platelets, 100 000/μL or less; prothrombin time, 80% or less; and indocyanine green retention rate after 15 minutes, 15% or more (Table 2).

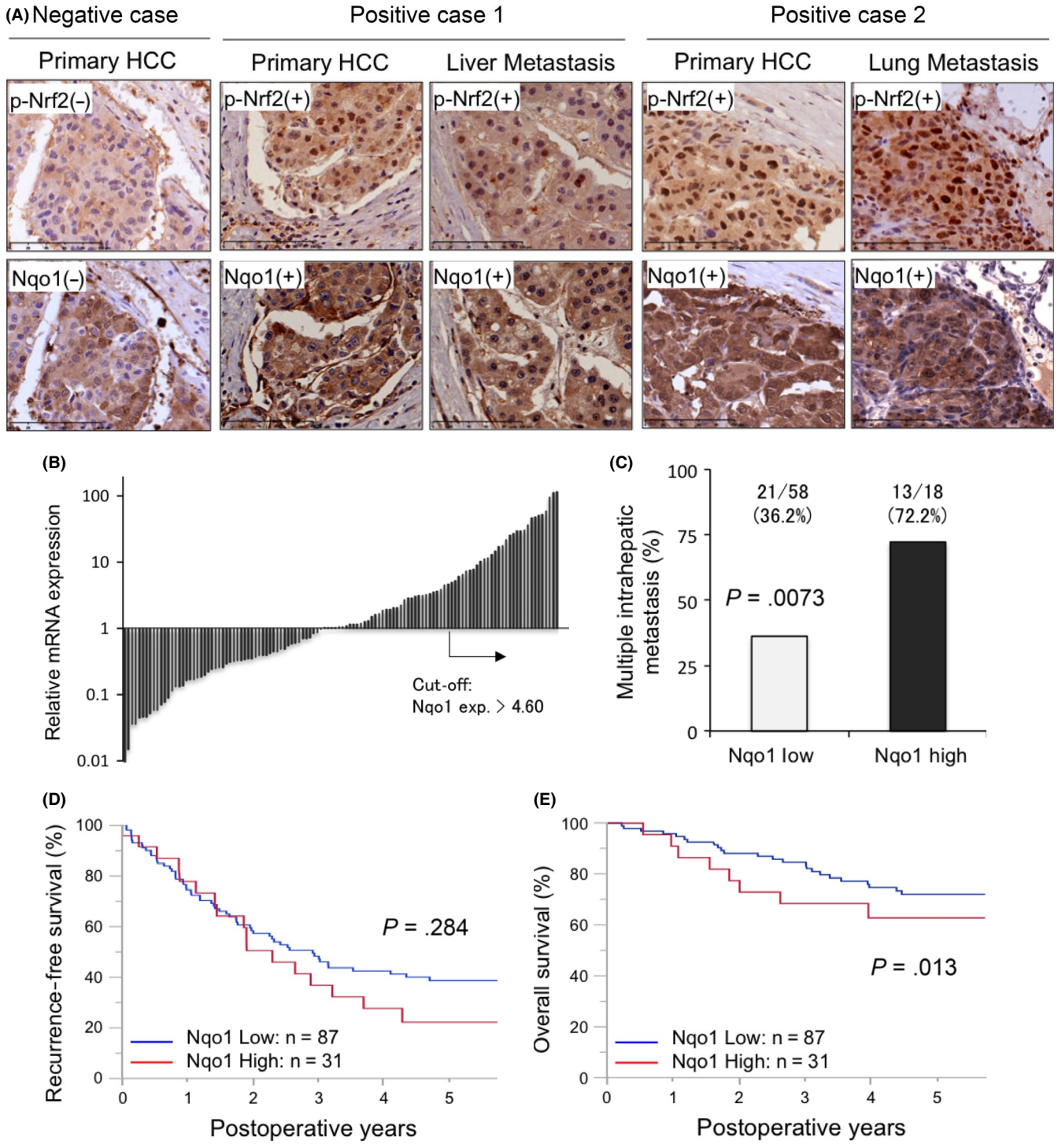

FIGURE 5 Elevated NADPH quinone oxidoreductase 1 (Nqo1) in hepatocellular carcinoma (HCC) tumors is associated with decreased overall survival. A, Representative sections from cases showing phosphorylated nuclear factor erythroid-derived 2-like 2 (p-Nrf2) in the nucleus and Nqo1 in the cytoplasm. B, Waterfall plot for the relative Nqo1 mRNA expression in the primary HCC lesion in the curative hepatectomy cohort. The quartile-bound cut-off (exp.> 4.60) was used to categorize high and low Nqo1 expression groups. C, Incidence of multiple intrahepatic recurrences was 2-fold higher in the Nqo1 high expression group (P = .0073). D, E, Kaplan-Meier analysis of recurrence-free survival (D) and patient overall survival (E) based on tumor Nqo1 expression levels in the curative hepatectomy cohort. Patients were grouped into Nqo1 low and high expression groups based on a quartile-bound cut-off (B). Overall survival (E) was significantly worse in the Nqo1 high group

We confirmed the relationship between Nqo1 expression and HCC metastasis in another validation cohort with surgically resected intrahepatic recurrent lesions (Figure S4B), however, no significant difference was shown due to the limited number of cases (n = 17). As expected, the group with high Nqo1 expression in the primary site frequently presented Nqo1-positive expression

TABLE 1 Characteristics of patients with hepatocellular carcinoma who underwent hepatic resection

Factors	Nqo1 low (n = 87)	Nqo1 high (n = 31)	*P* value
Age (years)	66.2 ± 11.9	70.3 ± 8.0	.1600
Gender, male	64 (73.60)	24 (75.00)	.9700
HBV	14 (16.10)	8 (25.00)	.2900
HCV	52 (59.80)	17 (53.10)	.4300
ASH + NASH	19 (21.80)	7 (21.90)	.9900
ICG15R (%)	15.5 ± 8.0	13.8 ± 6.6	.3800
Total bilirubin (mg/dL)	0.76 ± 0.26	0.88 ± 0.35	.1000
Albumin (g/dL)	3.9 ± 0.4	4.0 ± 0.5	.4200
Platelets ($\times 10^4/\mu L$)	16.4 ± 7.7	15.9 ± 5.7	.5900
Prothrombin time (%)	88.7 ± 10.2	87.7 ± 9.3	.6300
AFP ≥ 100 ng/mL	17 (19.50)	12 (38.70)	.0390
PIVKA2 ≥ 100 AU/mL	30 (34.50)	19 (61.30)	.0110
Liver fibrosis, F4	29 (33.30)	6 (19.40)	.1300
Tumor size ≥ 3cm	43 (49.40)	24 (77.40)	.0170
Tumor number ≥ 2	2 (2.30)	2 (6.45)	.3000
Differentiation, poor	20 (23.00)	13 (41.90)	.0410
fc (+)	57 (65.50)	20 (64.50)	.6400
s (+)	47 (54.00)	19 (61.30)	.6900
vp (+)	26 (29.90)	16 (51.60)	.0480
vv (+)	15 (17.20)	6 (19.40)	.8900
va (+)	1 (1.15)	3 (9.68)	.0300
b (+)	2 (2.30)	4 (12.90)	.0270
im (+)	11 (12.60)	5 (16.10)	.6400
Any recurrence (n = 84)	63 (72.40)	21 (67.70)	.5600
Intrahepatic recurrence (n = 74)	58 (66.60)	16 (51.60)	.2300
Simple/multiple	37/21	5/13	.0073
Extrahepatic recurrence (n = 14)	10/63 (15.90)	4/21 (19.10)	.7400

AFP, α-fetoprotein; ASH, alcoholic steatohepatitis; b, bile duct invasion; fc, capsule formation; HBV, hepatitis B virus; HCV, hepatitis C virus; im, intrahepatic metastasis; ICG15R, indocyanine green retention rate after 15 minutes; NASH, nonalcoholic steatohepatitis; Nqo1, NADPH quinone oxidoreductase 1; PIVKA2, protein induced by vitamin K absence/antagonist II; s, invasion of the serosa; va, hepatic artery invasion; vp, portal vein invasion; vv, hepatic vein invasion. Data are shown as n (%) or mean ± SEM.

in the recurrent lesions (4/5, 80.0%). Notably, more than half of the patients with low Nqo1 expression group at the primary site showed positive Nqo1 expression in metastatic lesions (7/12, 58.3%). Collectively, these results emphasize the potential role of Nqo1 in the development of intrahepatic metastasis after curative resection of primary HCC.

4 | DISCUSSION

In this study, we showed that depleting Nqo1 in HCC cell lines effectively diminished anchorage-independent survival and suppressed the formation of tumor spheroids by increasing intracellular ROS. Furthermore, β-Lap increased ROS selectively in spheroid cells and diminished anoikis resistance by futilely stimulating the upregulated Nqo1 (Figure 6). Clinicopathologic study indicated that Nrf2/Nqo1 overexpression was frequently observed in primary human HCC tissues and was associated with a higher incidence of multiple intrahepatic recurrence and poor prognosis.

Recent studies in tumor spheroids showed that Nrf2 is activated in the early period of detached culture,[32] and the antioxidant response with HO1[33] or Nqo1[34] is required for anchorage-independent growth. Other studies have shown that Nrf2 and Nqo1 expressions are associated with advanced tumor characteristics and are involved with recurrence-free survival and overall survival.[14,26,27] However, the specific mechanism underlying the association between Nrf2/Nqo1 and poor prognosis in HCC has been unclear.

TABLE 2 Univariate and multivariate analyses of factors related to overall survival in patients with hepatocellular carcinoma who underwent hepatic resection (Cox proportional hazards analysis)

	Univariate			Multivariate		
Factors	**RR**	**95% CI**	***P* value**	**RR**	**95% CI**	***P* value**
Low liver function	1.40	0.70-2.79	.340			
AFP ≥ 100 ng/mL	1.96	1.04-3.67	.036	1.40	0.68-2.88	.3600
PIVKA2 ≥ 100 AU/mL	1.61	0.87-2.98	.130			
Tumor number, ≥ 2	2.49	0.89-6.99	.080			
Tumor size, ≥ 3 cm	1.07	0.58-1.99	.830			
Differentiation, poor	1.24	0.64-2.40	.52			
vp (+)	1.82	0.98-3.38	.057	2.22	1.01-4.91	.0490
vv (+)	2.02	1.01-4.03	.047	1.13	0.46-2.86	.7800
im (+)	4.35	2.21-8.58	.011	3.94	1.65-9.44	.0021
Intrahepatic rec., Single	1.30	0.67-2.52	.430			
Intrahepatic rec., Multiple	2.50	1.24-5.04	.010	1.41	0.65-3.10	.3900
Nqo1 (+)	2.49	1.16-5.33	.019	3.02	1.54-10.25	.0031

AFP, α-fetoprotein; CI, confidence interval; im, intrahepatic metastasis; Nqo1, NADPH quinone oxidoreductase 1; PIVKA2, protein induced by vitamin K absence/antagonist II; rec., recurrence; RR, relative risk; vp, portal vein invasion; vv, hepatic vein invasion.

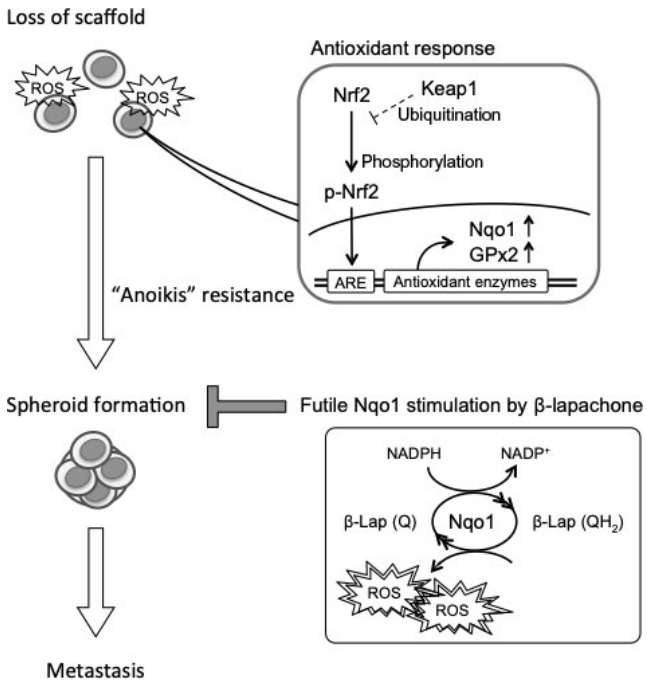

FIGURE 6 Cancer cells confronted with oxidative stress due to loss of scaffold and react with the nuclear factor erythroid-derived 2-like 2 (Nrf2)/ARE axis including NADPH quinone oxidoreductase 1 (Nqo1). Cells with anoikis resistance are able to build spheroid during circulation to the metastatic sites. β-Lapachone (β-Lap) futilely stimulates Nqo1 and induces excessive reactive oxygen species (ROS) to diminish the spheroid formation ability and prevent metastasis. GPx2, glutathione peroxidase-2; Keap1, Kelch-like ECH-associated protein 1; Q, quinone; QH_2, unstable hydroquinone; ARE, antioxidant response element

In the current study, we hypothesized that overexpression of the Nrf2/Nqo1 axis promotes HCC metastasis through anoikis resistance. We examined whether decreasing the elevated tumor Nqo1 levels would inhibit tumor survival using an in vitro 3D spheroid formation assay. Consistent with previous reports,[32,33,35] Nqo1 was upregulated at high levels during the early period of the detachment culture as a consequence of increased ROS and Nrf2 activation. We found that depleting Nqo1 increased ROS stress levels, significantly affected anchorage-independent survival of HCC cells, and reduced the size and number of spheroids. We also showed that silencing Keap1 promoted Nrf2/ Nqo1, reducing intracellular ROS and finally encouraging anchorage-independent survival and spheroid formation. These results indicated that Nqo1 plays a critical role in cancer cell sensitivity to anoikis, suggesting that modulating Nqo1 activity is of great importance to subjugate the metastatic process in HCC.

β-Lapachone stimulates Nqo1 to catalyze the oxidoreduction of β-lapachone (Q) to generate unstable hydroquinone (QH_2), then spontaneously regenerates the original compound, releasing massive ROS.[23] Thus, β-Lap stimulates the upregulated Nqo1 enzyme and increases ROS production, just like revving up the idling engine and increasing the exhaust CO_2 gas. Finally, unlike ordinal Nqo1 activation that lowers ROS, Nqo1 stimulation by β-Lap increases excessive ROS and induces apoptosis or anoikis. Here we showed the potent effect of β-Lap on increasing apoptotic cell death and suppressing spheroid formation selectively in Nqo1 upregulated HCC cells. Treatment with β-Lap increased intracellular ROS selectively in spheroid culture of control cells and diminished cell viability; in contrast, Nqo1 depletion increased intracellular ROS in spheroid culture but eliminated the sensitivity to β-Lap. These data suggest that stimulation of Nqo1 by β-Lap increases intracellular ROS and

detachment-induced cell death, depriving the metastatic potential of human HCC.

The prognoses of HCC patients are strongly influenced by frequent recurrence after curative resection[4]; treatment strategies for local recurrence and intrahepatic metastatic recurrence are major issues in improving the postoperative outcome of HCC.[36] Multiple intrahepatic recurrences lead to poor prognosis because of the limited resectability that is affected by the size, number, and distribution of recurrent lesions as well as individual hepatic reserve.[37] Our results showed that Nqo1 expression was associated with the occurrence of multiple intrahepatic recurrent lesions and was correlated with poor overall survival.

There was a limitation in our immunohistochemical analysis on our primary curative resection cohort; as the diagnoses of intrahepatic recurrences were undertaken with hemodynamic computed tomography/MRI exams, de novo carcinogenesis might be included at a certain rate. Even after deducting the possibility of de novo carcinogenesis, the frequency of multiple relapsed cases is considered to be sufficiently different between the Nqo1 high/low expression groups; however, more appropriate diagnostic criteria for relapse are required. Our study also showed that Nqo1 overexpression was frequently observed in the intrahepatic recurrent lesions, including the Nqo1-negative cases at the primary site. This indicates that dispatched HCC cells have possibly acquired p-Nrf2/Nqo1 activity while circulating to the metastatic sites. We are currently investigating the potential role of histone methylation in epigenetically inducing anoikis resistance acquisition (Shimokawa M. et al, unpublished data). Our validation cohort also had limitations, as recurrent lesions were pathologically identified and the number of re-resected cases is statistically insufficient. Recent studies reported that molecular and immunological discrimination of multicentric occurrences and intrahepatic metastasis can be undertaken by multiplatform analysis using indicators such as gene mutation patterns and DNA methylation patterns.[38,39] Future studies should introduce such techniques and increase the number of cases for more precise analysis.

Our clinical results also suggested that Nqo1 levels increase during the process of metastasis, indicating that cancer cells induce Nqo1 expression as part of a survival strategy during metastasis. Considering the very low survival rate in early suspension culture under β-Lap treatment, this novel drug could effectively eradicate the dispatched HCC cells from the primary site and suppress intrahepatic or distant metastasis. Contrary to the remarkable cytotoxicity of β-Lap in Nqo1 upregulated sphere cells, Nqo1 depleted cells showed the high viability against even higher concentration of β-Lap (5-10 μmol/L), suggesting that the cytotoxicity is also weak to normal hepatocytes. Furthermore, β-lapachone kills cancer cells regardless of cell cycle position[25] and synergizes with selective chemotherapies[40] and radiation therapies.[41] β-Lapachone is now considered to be a promising drug from the viewpoint of patient safety, and is expected to be effective as an adjuvant therapy after hepatectomy. Further studies are necessary including animal experiments on the cytotoxicity during the liver regeneration phase after hepatectomy.

In conclusion, here we showed that Nqo1 activation was related to metastasis and poor prognosis by enabling HCC cells to overcome anoikis during anchorage-independent culture. Our findings could provide a new therapeutic approach for the prevention of postoperative HCC recurrence.

ACKNOWLEDGMENTS

The authors would like to thank Ms Saori Tsurumaru, Ms Asuka Nakamura, Ms Yuko Kubota, and Ms Miki Nakashima for their technical support. We thank Edanz Group for editing a draft of this manuscript. This study was supported by the following 2 grants: JSPS KAKENHI, Grant-in-Aid from the Ministry of Health, Labour and Welfare, Japan (Nos. JP-16K10576 and 19K09198). The funding sources had no role in the collection, analysis, or interpretation of the data, or in the decision to submit the article for publication.

CONFLICT OF INTEREST

The authors have no conflicts of interest to declare.

ORCID

Shinji Itoh https://orcid.org/0000-0003-0382-2520
Kyohei Yugawa https://orcid.org/0000-0001-5121-682X

REFERENCES

1. Llovet JM, Zucman-Rossi J, Pikarsky E, et al. Hepatocellular carcinoma. *Nat Rev Dis Primers*. 2016;2:16018.
2. Ghouri YA, Mian I, Rowe JH. Review of hepatocellular carcinoma: Epidemiology, etiology, and carcinogenesis. *J Carcinog*. 2017;16:1.
3. El-Serag HB, Rudolph KL. Hepatocellular carcinoma: epidemiology and molecular carcinogenesis. *Gastroenterology*. 2007;132:2557-2576.
4. Poon RT, Fan ST, Lo CM, Liu CL, Wong J. Intrahepatic recurrence after curative resection of hepatocellular carcinoma: long-term results of treatment and prognostic factors. *Ann Surg*. 1999;229:216-222.
5. Eccles SA, Welch DR. Metastasis: recent discoveries and novel treatment strategies. *Lancet*. 2007;369:1742-1757.
6. Chambers AF, Groom AC, MacDonald IC. Dissemination and growth of cancer cells in metastatic sites. *Nat Rev Cancer*. 2002;2:563-572.
7. Bhowmick NA, Neilson EG, Moses HL. Stromal fibroblasts in cancer initiation and progression. *Nature*. 2004;432:332-337.
8. Giannoni E, Chiarugi P. Redox circuitries driving Src regulation. *Antioxid Redox Signal*. 2014;20:2011-2025.
9. Piskounova E, Agathocleous M, Murphy MM, et al. Oxidative stress inhibits distant metastasis by human melanoma cells. *Nature*. 2015;527:186-191.
10. Taddei ML, Giannoni E, Fiaschi T, Chiarugi P. Anoikis: an emerging hallmark in health and diseases. *J Pathol*. 2012;226:380-393.
11. Gorrini C, Harris IS, Mak TW. Modulation of oxidative stress as an anticancer strategy. *Nat Rev Drug Discov*. 2013;12:931-947.
12. Itoh K, Wakabayashi N, Katoh Y, Ishii T, O'Connor T, Yamamoto M. Keap1 regulates both cytoplasmic-nuclear shuttling and degradation of Nrf2 in response to electrophiles. *Genes Cells*. 2003;8:379-391.
13. Taguchi K, Motohashi H, Yamamoto M. Molecular mechanisms of the Keap1-Nrf2 pathway in stress response and cancer evolution. *Genes Cells*. 2011;16:123-140.
14. DeNicola GM, Karreth FA, Humpton TJ, et al. Oncogene-induced Nrf2 transcription promotes ROS detoxification and tumorigenesis. *Nature*. 2011;475:106-109.
15. Niture SK, Jain AK, Jaiswal AK. Antioxidant-induced modification of INrf2 cysteine 151 and PKC-delta-mediated phosphorylation of Nrf2 serine 40 are both required for stabilization and nuclear

translocation of Nrf2 and increased drug resistance. *J Cell Sci*. 2009;122:4452-4464.
16. Jain AK, Jaiswal AK. Phosphorylation of tyrosine 568 controls nuclear export of Nrf2. *J Biol Chem*. 2006;281:12132-12142.
17. Mitsuishi Y, Taguchi K, Kawatani Y, et al. Nrf2 redirects glucose and glutamine into anabolic pathways in metabolic reprogramming. *Cancer Cell*. 2012;22:66-79.
18. Schafer ZT, Grassian AR, Song L, et al. Antioxidant and oncogene rescue of metabolic defects caused by loss of matrix attachment. *Nature*. 2009;461:109-113.
19. Jiang L, Shestov AA, Swain P, et al. Reductive carboxylation supports redox homeostasis during anchorage-independent growth. *Nature*. 2016;532:255-258.
20. Itoh S, Maeda T, Shimada M, et al. Role of expression of focal adhesion kinase in progression of hepatocellular carcinoma. *Clin Cancer Res*. 2004;10:2812-2817.
21. Huang X, Dong Y, Bey EA, et al. An NQO1 substrate with potent antitumor activity that selectively kills by PARP1-induced programmed necrosis. *Cancer Res*. 2012;72:3038-3047.
22. Blanco E, Bey EA, Khemtong C, et al. Beta-lapachone micellar nanotherapeutics for non-small cell lung cancer therapy. *Cancer Res*. 2010;70:3896-3904.
23. Bey EA, Bentle MS, Reinicke KE, et al. An NQO1- and PARP-1-mediated cell death pathway induced in non-small-cell lung cancer cells by beta-lapachone. *Proc Natl Acad Sci U S A*. 2007;104:11832-11837.
24. Huang X, Motea EA, Moore ZR, et al. Leveraging an NQO1 bioactivatable drug for tumor-selective use of poly(ADP-ribose) polymerase inhibitors. *Cancer Cell*. 2016;30:940-952.
25. Pink JJ, Planchon SM, Tagliarino C, Varnes ME, Siegel D, Boothman DA. NAD(P)H: Quinone oxidoreductase activity is the principal determinant of beta-lapachone cytotoxicity. *J Biol Chem*. 2000;275:5416-5424.
26. Solis LM, Behrens C, Dong W, et al. Nrf2 and Keap1 abnormalities in non-small cell lung carcinoma and association with clinicopathologic features. *Clin Cancer Res*. 2010;16:3743-3753.
27. Kawasaki Y, Okumura H, Uchikado Y, et al. Nrf2 is useful for predicting the effect of chemoradiation therapy on esophageal squamous cell carcinoma. *Ann Surg Oncol*. 2014;21:2347-2352.
28. Ma Y, Kong J, Yan G, et al. NQO1 overexpression is associated with poor prognosis in squamous cell carcinoma of the uterine cervix. *BMC Cancer*. 2014;14:414.
29. Yang Y, Zhang Y, Wu Q, et al. Clinical implications of high NQO1 expression in breast cancers. *J Exp Clin Cancer Res*. 2014;33:14.
30. Itoh S, Taketomi A, Tanaka S, et al. Role of growth factor receptor bound protein 7 in hepatocellular carcinoma. *Mol Cancer Res*. 2007;5:667-673.
31. Itoh S, Taketomi A, Harimoto N, et al. Antineoplastic effects of gamma linolenic Acid on hepatocellular carcinoma cell lines. *J Clin Biochem Nutr*. 2010;47:81-90.
32. Ryoo IG, Choi BH, Kwak MK. Activation of NRF2 by p62 and proteasome reduction in sphere-forming breast carcinoma cells. *Oncotarget*. 2015;6:8167-8184.
33. Dey S, Sayers CM, Verginadis II, et al. ATF4-dependent induction of heme oxygenase 1 prevents anoikis and promotes metastasis. *J Clin Invest*. 2015;125:2592-2608.
34. Madajewski B, Boatman MA, Chakrabarti G, Boothman DA, Bey EA. Depleting Tumor-NQO1 potentiates anoikis and inhibits growth of NSCLC. *Mol Cancer Res*. 2016;14:14-25.
35. Cheng X, Liu F, Liu H, Wang G, Hao H. Enhanced glycometabolism as a mechanism of NQO1 potentiated growth of NSCLC revealed by metabolomic profiling. *Biochem Biophys Res Commun*. 2018;496:31-36.
36. Erridge S, Pucher PH, Markar SR, et al. Meta-analysis of determinants of survival following treatment of recurrent hepatocellular carcinoma. *Br J Surg*. 2017;104:1433-1442.
37. Tabrizian P, Jibara G, Shrager B, Schwartz M, Roayaie S. Recurrence of hepatocellular cancer after resection: patterns, treatments, and prognosis. *Ann Surg*. 2015;261:947-955.
38. Furuta M, Ueno M, Fujimoto A, et al. Whole genome sequencing discriminates hepatocellular carcinoma with intrahepatic metastasis from multi-centric tumors. *J Hepatol*. 2017;66:363-373.
39. Shimada S, Mogushi K, Akiyama Y, et al. Comprehensive molecular and immunological characterization of hepatocellular carcinoma. *EBioMedicine*. 2019;40:457-470.
40. Li CJ, Li YZ, Pinto AV, Pardee AB. Potent inhibition of tumor survival in vivo by beta-lapachone plus taxol: combining drugs imposes different artificial checkpoints. *Proc Natl Acad Sci U S A*. 1999;96:13369-13374.
41. Park HJ, Ahn KJ, Ahn SD, et al. Susceptibility of cancer cells to beta-lapachone is enhanced by ionizing radiation. *Int J Radiat Oncol Biol Phys*. 2005;61:212-219.

SUPPORTING INFORMATION

Additional supporting information may be found online in the Supporting Information section.

How to cite this article: Shimokawa M, Yoshizumi T, Itoh S, et al. Modulation of Nqo1 activity intercepts anoikis resistance and reduces metastatic potential of hepatocellular carcinoma. *Cancer Sci*. 2020;111:1228–1240. https://doi.org/10.1111/cas.14320